Journal of Testing and Evaluation, Nov. 2003, Vol. 31, No. 6
Paper ID JTE11805_316
Available online at www. astm.org

A. F. M. S. Amin,[1] *M. S. Alam,*[2] *and Y. Okui*[3]

Measurement of Lateral Deformation in Natural and High Damping Rubbers in Large Deformation Uniaxial Tests

ABSTRACT: In testing the mechanical behavior of rubbers, the incompressibility assumption is used to predict the deformed cross section under loading and thereby to calculate the true stress. There are, however, cases where rubbers can undergo considerable volumetric deformation in large strain experiments. Microstructural investigation through a scanning electron microscope was carried out on a void-filled natural rubber specimen to clarify the effect of voids on the compressibility feature. The microstructure of the natural rubber was observed qualitatively and quantitatively in uniaxial tension and compared to the microstructure in the undeformed condition. The existence of the compressibility feature in the void-filled rubber was confirmed from a microstructural viewpoint. The findings indicate the necessity of accurate measurement of the deformed cross section in mechanical tests to obtain the true stress. To this end, an experimental setup capable of measuring the deformed cross section of the rubber specimens subjected to large uniaxial compression is proposed. To do this, the accuracy of laser beams is used for measurement of distance and a mechanical jig is developed to synchronize the movement of the laser transducer with the vertical crosshead of the load cell of a computer-controlled servohydraulic testing machine. Thus the constraints associated with conventional strain gages in measuring large strains are overcome. Finally, two natural rubber specimens and one high damping rubber specimen were tested in the proposed setup to display the adequacy of the developed device in measuring lateral deformation of rubber-like highly deformable solids in large strain uniaxial testing.

KEYWORDS: incompressibility, large deformation, void-filled microstructure, lateral deformation measurement, uniaxial test, natural rubber, high damping rubber

Introduction

Natural gum rubber is derived from natural sources. It falls in the class of polymeric materials. However, such rubber is unsuitable for engineering applications and it therefore needs vulcanization treatment. During the treatment, carbon black particles are added as filler together with some sulfur and other elements to create crosslink bonds within the molecular chains of the polymer. Such treatment changes the rubber microstructure and improves some of its mechanical properties [1–3]. Vulcanized natural rubbers are now widely used as shock absorbers, mounts, bridge bearings, seals, wind shoes, and tunnel linings. Recently, high damping rubber has been developed for base isolation bearings that protect structures from earthquakes [4].

The bulk modulus of a solid rubber is usually very large and it is larger by several orders of magnitude than the shear modulus. Hence rubber is called an incompressible material. When an incompressible material is subjected to uniaxial stretch (λ_1), the relationship of the positions in undeformed and deformed configurations is described by the following deformation gradient tensor **F** [5–7]:

$$F_{ij} = \begin{pmatrix} \lambda_1 & 0 & 0 \\ 0 & \lambda_2 & 0 \\ 0 & 0 & \lambda_3 \end{pmatrix} = \begin{pmatrix} \frac{l}{l_0} & 0 & 0 \\ 0 & \sqrt{\frac{l_0}{l}} & 0 \\ 0 & 0 & \sqrt{\frac{l_0}{l}} \end{pmatrix} = \begin{pmatrix} \lambda_1 & 0 & 0 \\ 0 & \sqrt{\frac{1}{\lambda_1}} & 0 \\ 0 & 0 & \sqrt{\frac{1}{\lambda_1}} \end{pmatrix} \quad (1)$$

where

$\lambda_1, \lambda_2, \lambda_3$ = stretches in three principal directions;
$\lambda_1 \lambda_2 \lambda_3 = 1$, meets the condition of incompressibility;
l = the length of the specimen at time t: $l = l(t)$,
$l_0 = l$ at $t = 0$.

Equation 1 shows a way of predicting lateral deformation (F_{22} and F_{33}) of an incompressible material by knowing F_{11} from uniaxial tests. The deformed cross section perpendicular to the loading direction can be calculated from this expression, and is traditionally used to calculate the Cauchy (true) stress [8–10].

However, earlier works indicated that there are cases where voids can remain present in rubber microstructure. Cornwell and

Manuscript received 11/21/2002;accepted for publication 6/10/2003;published 11/01/2003.

[1] Department of Civil Engineering, Bangladesh University of Engineering and Technology, Dhaka 1000, Bangladesh.
[2] Hyundai Engineering and Construction Co., Ltd, Dhaka Braner, House 12, Road 111, Gulshar 2, Dhaka 1212, Bangladesh.
[3] Department of Civil and Environmental Engineering, Saitama University, 255 Shimo Okubo, Saitama 338-8570, Japan.

Copyright © 2003 by ASTM International, 100 Barr Harbor Drive, PO Box C700, West Conshohocken, PA 19428-2959.

Schapery [11] studied the fracture of particulate-filled rubber materials in tension through a Scanning Electron Microscope (SEM). In the study, a role of existing voids in the fracture process was clarified through SEM observation. In addition, Hermann et al. [12, 13] reported the possibility of the effect of microstructural voids on the incompressibility property. Recently, Amin et al. [14] and Amin [15] presented some SEM micrographs of different natural rubber and high damping rubber specimens, where the existence of microvoids was detected. It is apprehended that these rubbers with voided microstructure may suffer from volumetric deformation upon external loading. Hence, the validity of incompressibility assumption used for calculating the true stress (Cauchy stress) may be subject to question. This indicates the necessity of measuring lateral deformation for acquiring the exact stress-strain relationship.

To address this problem, Kugler et al. [16] used a direct optical measurement technique to measure the lateral strain and Poisson's ratio in tension experiments. Later, Fishman and Machmer [17] investigated the capability of three possible test setups for bulk modulus determination. These were named the deformation jacket method, volume change device method, and piston method. In another effort, Migwi et al. [18] used thermal mechanical analysis measurement equipment to measure the shear modulus and Poisson's ratio and also studied the effect of temperature on these parameters. Peng et al. [19] proposed an inexpensive testing method, where a rubber disk can be tested in a fully confined condition achieved by using a metal jacket. Nevertheless, it is worthwhile to mention here that the primary motivation for proposing these experimental methods was to measure Poisson's ratio, which is only meaningful in small strain cases.

In contrast, due to large deformations (in a range of 50 % strain or more), conventional strain gages fail to measure the strains. This indicates the necessity of an optical measurement of the displacement normal to the loading direction. In optical measurement techniques, another problem arises due to the significant shift of the measurement plane caused by a very large applied displacement. However, no work is reported until now for a direct measurement of the deformed cross section of a specimen that is subjected to a large strain. In such a situation, Arruda and Boyce [20], Lion [21], Boyce and Arruda [22] depended on engineering stress (nominal stress) calculated on the basis of initial cross section to present the experimental results. The standard procedure for testing rubber in uniaxial tension (ASTM D 412-98a [23]) suggests a way for measuring nominal stress, but it does not suggest any way for measuring the true stress. On the other hand, Anand [24] and Peng and Cheng [25] indicate lack of published experimental findings for validation of their theoretical models for compressible rubbers.

With this background, the paper compares the SEM micrographs of a void-filled natural rubber specimen in an undeformed state and under uniaxial tension. An image analysis technique is used to quantify the void area ratios of the specimen at different strain magnitudes to show the effect of strain amplitude on the compressibility. A mechanical test setup capable of measuring the lateral deformation in a large strain uniaxial compression test is presented. The measured lateral stretch and the corresponding Cauchy stress-stretch relations are compared with those obtained from the incompressibility assumption. Results obtained from three different specimens with different microstructures are presented to display the applicability of the device to varied material types.

Specimens

Two types of natural rubber specimens (NR-I and NR-II) and one high damping rubber (HDR) specimen are used in the present work. Table 1 shows the details of the specimens. The earlier preliminary study on rubber microstructure [14] has shown that the NR-I contains a significant amount of microvoids, while in the other two specimens void presence is very rare. The presence of microvoids in NR-I is therefore addressed in more detail in the current work through qualitative and quantitative SEM observation to learn their effect on microstructural deformation. However, due to the scarce presence of voids in NR-II and HDR, no information on microstructure could be gathered from the present SEM study.

Change of NR-I Microstructure Under In Situ Tension

SEM observations were performed to study the microstructure of NR-I in the undeformed state and under in situ tension. Observations were made using a computer-controlled SEM apparatus (Jeol JSM 5600LV). Specially prepared samples of the specimens were placed in the SEM chamber after preliminary treatment.

Sample Preparation

Specimens (approximately 3 mm $\times$ 5 mm $\times$ 1.5 mm) were prepared from the rubber blocks. A very sharp cutting edge and the same cutting method were used for all specimens. Comparative observations were made. Undeformed samples were mounted on the SEM chamber using double-sided adhesive tapes. However, in case of applying in situ tension, glue was used to mount the specimens at their edges. Ink marks were used to measure the applied strain. After mounting, the samples were coated with a conductor to ensure an electron-conducting path for the electron beam. A gold-palladium coating was applied by using a vacuum evaporator (Jeol JFC 1200 Fine Coater) operated at a pressure of 8 Pa for 45 s.

TABLE 1—*Details of the specimens.*

	Specimen Designation		
	NR-I	NR-II	HDR
Application	General purpose	Bridge bearing	Bridge bearing
Manufacturer	Shinoda Rubber Co.	Yokohama Rubber Co.	Yokohama Rubber Co.
Strength	4.0 MPa*	0.98 MPa**	0.78 MPa**
Shape	Cubic	Cylindrical	Cylindrical
Size	H:50 mm, L:50 mm, W:50 mm	H:41 mm, D:49 mm	H:41 mm, D:49 mm

H: Height, L: Length, W: Width, D: Diameter, T: Thickness. * Tensile strength, ** Shear modulus tested according to JIS K 6301.

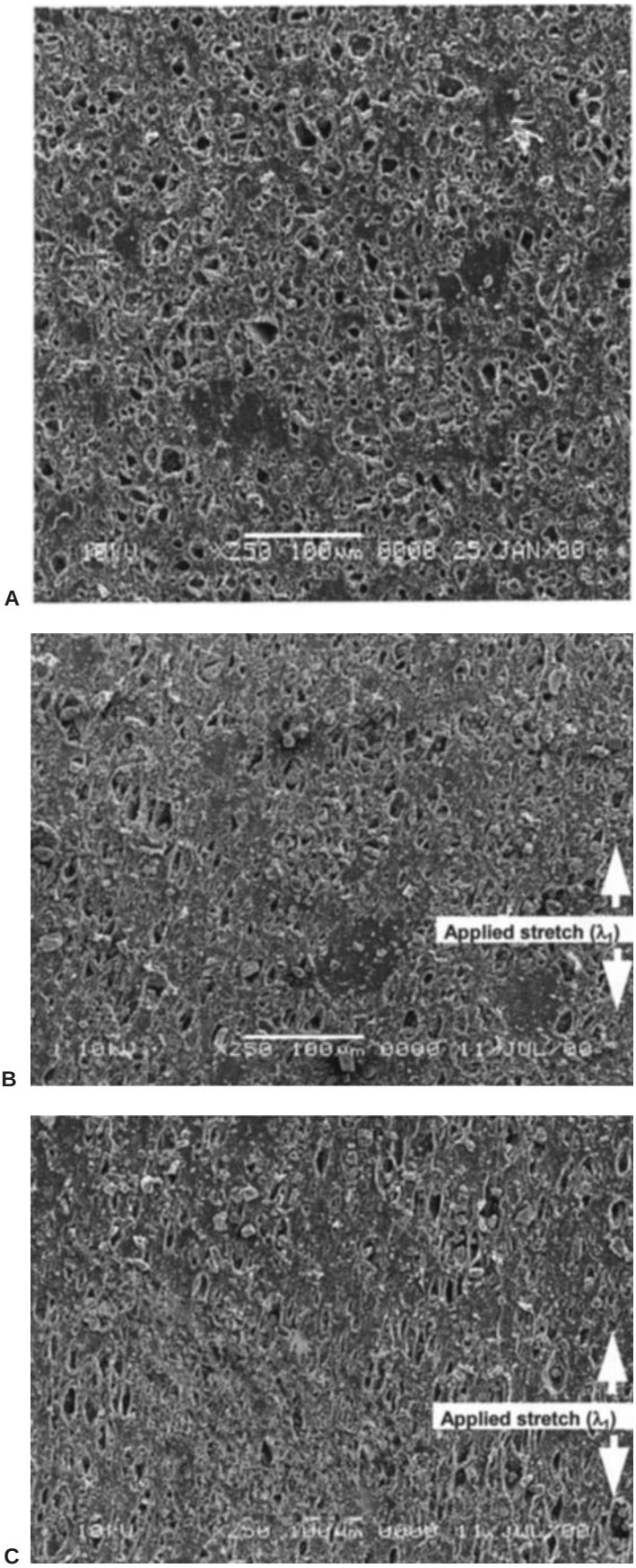

FIG. 1—*SEM micrographs of NR-I. (a) At undeformed state, (b) At 1.2 stretch level, (c) At 1.4 stretch level.*

Observations

The SEM image was viewed on a monitor and it was captured as bitmap data using a personal computer. The observations were done on undeformed specimens as well as on specimens under in situ tension at 1.2 and 1.4 stretch (giving 20 % and 40 % engineering strain) levels. Figure 1 presents the photomicrographs of NR-I in the virgin state and under in situ tension. The figures clearly show the presence of a significant number of voids in the microstructure that change in shape with application of stretch. Here the voids are found to transform from a circular shape to a completely elliptical shape and to orient in the stretching direction with increasing applied tensile stretch. The change in void shape can be attributed to the application of tensile displacement. The voids extend in the stretching axis (associated with λ_1) and are compressed in the two other axes (associated with λ_2 and λ_3). The orientation of voids along the direction of applied stretching can be noted from the figure. This phenomenon also hints at the situation that voids may experience in the case of applying compressive stretch, which is difficult to observe in the SEM. In such a case, the applied compressive stretch in one axis (associated with λ_1) causes a tension stretch in the other two axes (associated with λ_2 and λ_3). This action will be further discussed when presenting the mechanical test results in uniaxial compression.

Void Area Measurement

The samples were observed in different magnifications for precise measurements of the ratio of void area on a cross section. The observations were made at the middle of the specimen to minimize the boundary effects. Measurements of comparative void areas in undeformed specimens and in situ tension specimens were made using an image processing and analysis program (Scion Image 2000 [26]). To obtain representative values from the measurements, four independent calculations were done. The average values were then recorded. The variations between the calculations were found to be within 0.7 %. The comparative voids measured from the SEM photographs are listed in Table 2. The values show that void area ratio decreases with increasing applied tension. This indicates the compressibility feature in the void phase of the material at higher stretch levels. On the basis of mechanical test results, this observation will be further clarified in the later part of this paper.

Mechanical Test Setup in Compression

The objective of developing the test setup was to measure the deformed cross section of a rubber specimen subjected to large uniaxial compressive strains of the order of 50 %. Displacement was applied in the vertical direction (associated with λ_1) on the specimen that resulted in extension in the other two directions (associated with λ_2 and λ_3). To do this, a computer-controlled servohydraulic testing machine was used for loading the specimen. A laser transducer was used to measure the deformed cross section. A mechanical device was devised to synchronize the laser device movement with the movement of load cell crosshead. Measures were

TABLE 2—*Measured void area ratios in NR-I.*

Specimens	Void Area Ratio (%)
Undeformed	15.7 ± 0.7
Deformed under in situ tension (1.2 stretch level)	15.1 ± 0.7
Deformed under in situ tension (1.4 stretch level)	14.2 ± 0.6

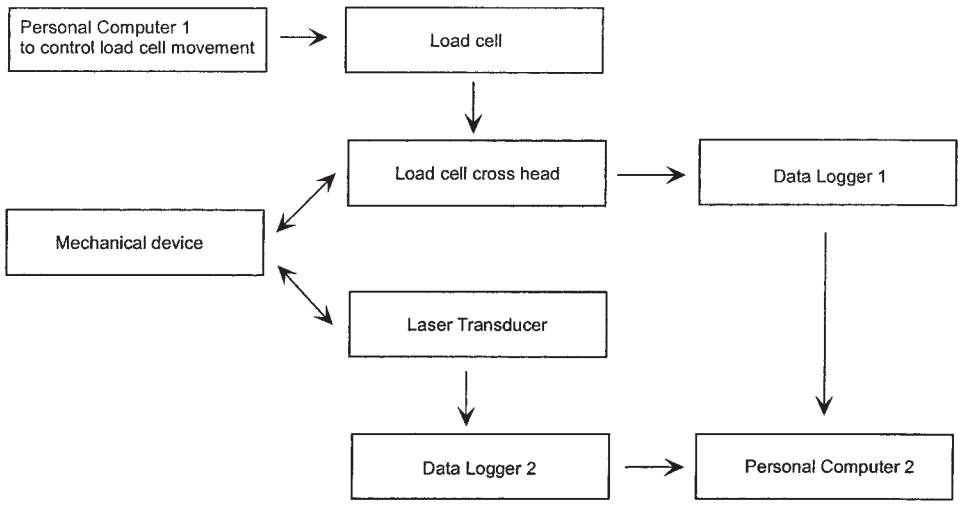

FIG. 2—*Schemetic flow chart of mechanical test setup.*

taken to obtain a homogeneous deformation in the specimen by reducing friction between the plates and the specimens to the minimum. Figure 2 shows a schematic chart of the setup.

Load Cell

A computer-controlled servohydraulic testing machine (Shimadzu Servo Pulser 4800) was used with a load cell of 20-ton capacity to apply displacement. The maximum stroke rate of the load cell cross head was 50 mm/s. Displacement was applied in the vertical direction on the specimen and the corresponding reaction was obtained from the load cell as load.

Lateral Deformation Measurement Using Laser Transducer

Rubbers are relatively soft materials that undergo large deformation upon loading. In the large deformation range, conventional strain gages, having limited strain-measuring capacity, fail to give any strain values. Furthermore, any conventional strain-measuring device is required to be physically attached to the specimen. However, due to the soft nature of the material undergoing large deformation, the strain gage itself causes local deformation of the specimen. To overcome all these problems, an optical measurement technique was adopted. The accurate laser beam was used for precise measurement of lateral displacement of the specimen at its midheight. This opens the way for evaluating Cauchy stress (true stress) at a cross section perpendicular to the direction of loading. In the current work, a laser transducer (Ono Sokki LD-1110M-020) having a measurement range of 100 mm was used. The transducer uses laser rays of 3B class with 0.6 mm resolution. However, due to the application of large vertical displacement to obtain a compressive strain of around 50 %, the midheight point of the deformed specimen shifts significantly from its undeformed location and the laser transducer fails to catch the target point. To overcome this problem, a special mechanical device was designed and constructed to synchronize the laser ray movement in the vertical direction with the vertical movement of the load cell crosshead.

Mechanical Device for Controlling Laser Transducer Movement

The mechanical device consists of three horizontal plates, namely a fixed top plate, a movable load transfer plate, and a fixed bottom plate framed in two stiff vertical columns. An integrated system consisting of boom, horizontal bar, slider channel, and slider ring was designed to control the synchronous movement of a laser transducer. To minimize the friction and thereby ensure friction free movement, the moving components were made from smooth-surfaced stainless steel. Some additional lubricants also were used with the moving components. Figures 3–5 show the details of the device.

Fixed Top and Bottom Plates—The bottom plate is a solid plate and it is attached to the bottom frame of the testing machine to support the specimen. The top plate, however, contains a circular opening and allows the free movement of the load cell crosshead.

Stiff Vertical Columns—Two vertical columns are attached to the fixed top and bottom plates. The columns are made of smooth stainless steel to allow friction-free movement of the load transfer plate and the slider rings.

Load Transfer Plate and Slider Rings—This is the plate where the vertical crosshead of the load cell rests. The plate allows the transfer of load to the specimen. It is attached to stainless steel slider rings, which are capable of moving through the vertical columns.

Boom, Horizontal Bar, and Slider Channel—The boom is made of four steel limbs hinged at each end. One end of each of these limbs is hinged either with the load transfer plate or the fixed bottom plate. The other remaining ends of these limbs are hinged and finally attached to a stainless steel horizontal bar through a special sliding ring. The ring allows only horizontal movement of the horizontal bar and restricts vertical movement (Fig. 4). One end of the horizontal bar is attached to a sliding channel and an L-cross sectioned fixing plate to fix the laser transducer. The vertical reaction produced by the special sliding ring on the horizontal bar is transferred to the L-shaped fixing plate causing its vertical movement. The sliding channel allows the friction-free movement of the fixing plate along with the laser transducer in the vertical plane while preventing any movement in the horizontal direction.

Stopper—To prevent any damage to the boom and its other accessories due to the accidental excess application of vertical displacement, a steel block is fixed to the bottom plate.

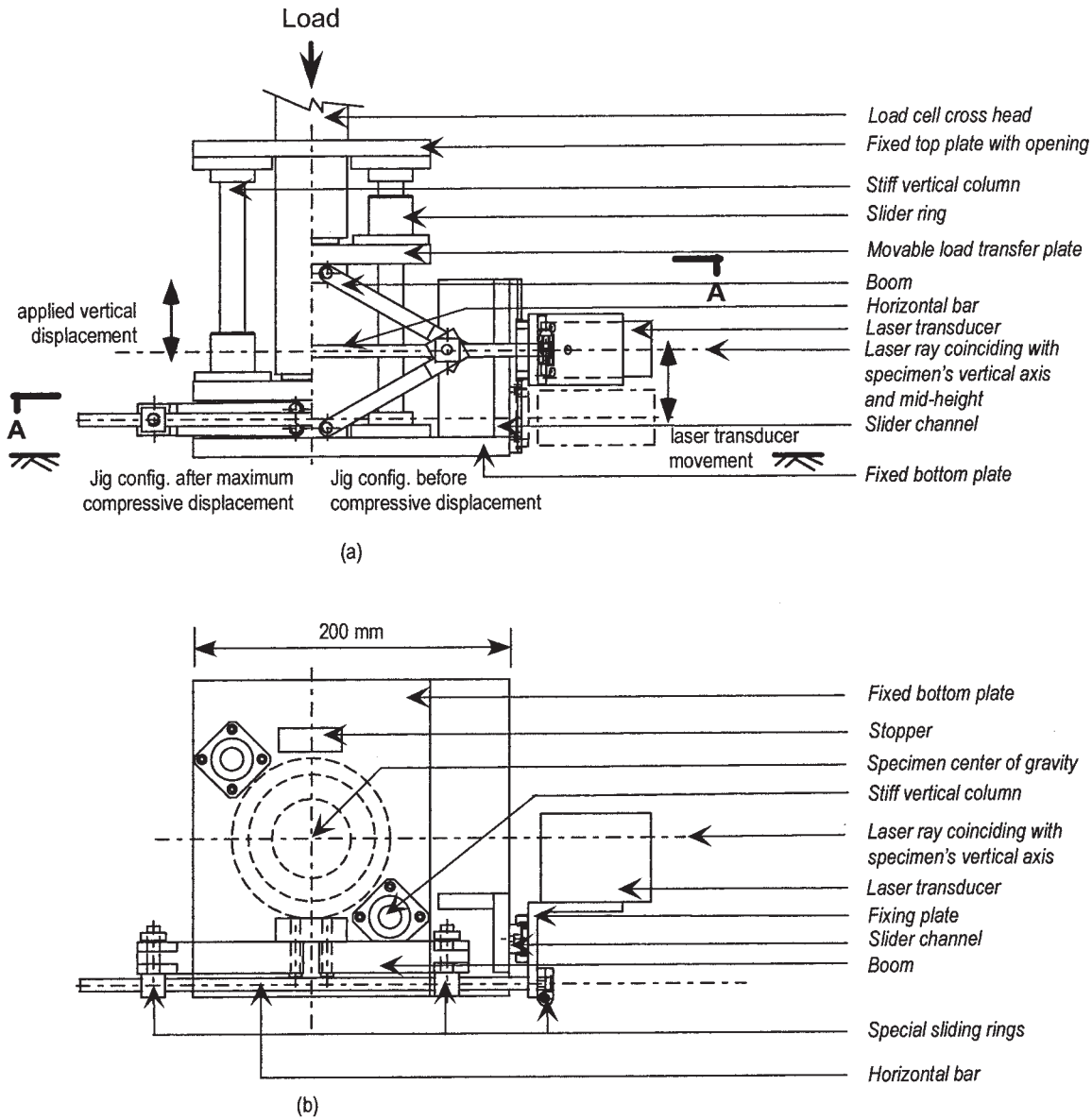

FIG. 3—*Details of mechanical device for synchronized laser transducer movement. (a) Elevation; (b) Plan view at Section A-A.*

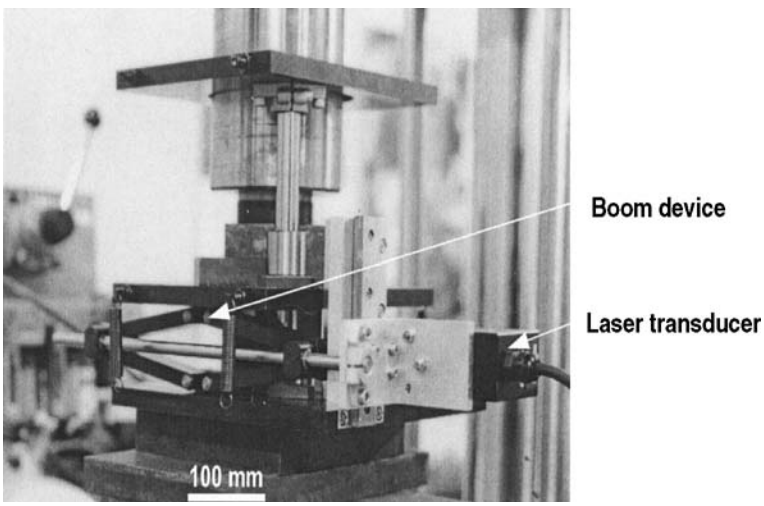

FIG. 4—*Photograph showing the mechanical device and laser transducer.*

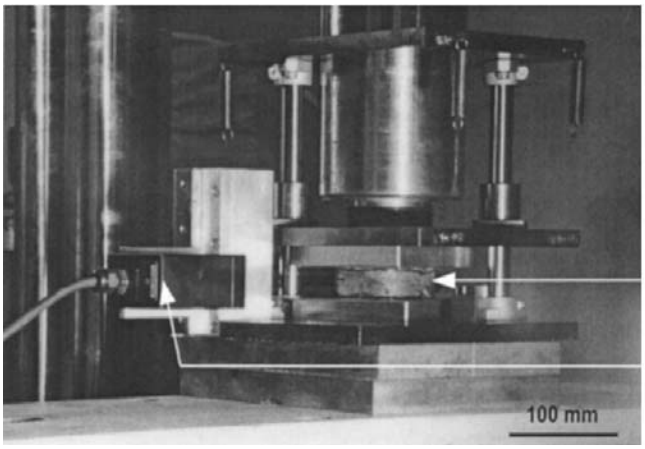

FIG. 5—*Photograph showing the laser transducer and the mechanical device with a specimen at 50 % compressive strain. The attainment of deformation homogeneity can be noted.*

Centering—In the laser displacement measurement, the centering of the specimen in the direction of loading and the alignment of the specimen along the laser beam are very important. Figure 3*b* illustrates the coincidence of the location of the center of gravity of the specimen with the path of the laser beam. It is obvious that the size and dimensions of the laser transducer dominate the design of the whole system (Fig. 5). The dotted circular rings (Fig 3*b*) indicate the crosshead location and the probable extent of areas that a cylindrical specimen can laterally occupy in a deformed state.

Reducing Friction Between the Specimen and Plates and Attainment of Homogeneous Deformation in the Specimen—This is the other important aspect of the test setup. To this end, poly(propylene) sheets at the top and at the bottom surface of the specimen along with lubricants were used to cut the friction between the movable load transfer plate, fixed bottom plate, and the specimen surfaces. Figure 5 illustrates the deformation homogeneity achieved at 50 % compressive strain. The attainment of homogeneous specimen deformation allowed considering F_{22} and F_{33} values to be equal in calculating the deformed cross sectional area.

Mechanical Test Results in Compression

The experimental setup presented in the last section was used to test the mechanical behavior of NR-I, NR-II, and HDR under monotonic compression. Tests were performed at room temperature on preloaded specimens after removing Mullins' effect (Mullins [27]). A five cycle preloading up to 0.5 stretch level was applied at a stretch rate of 0.1/s. Such preloading is commonly practiced for removing Mullins' effect from other phenomena and was followed by Yeoh [28], Yamashita and Kawabata [29], Lion [21,30], Bergstrom and Boyce [8], Miehe and Keck [31], and Amin et al. [14]. The specimens were stretched in the vertical direction (λ_1), while the lateral stretch (λ_2) was measured using the proposed test setup. The lateral stretches and the calculated Cauchy stresses as obtained from the direct lateral cross section measurement and those from the incompressibility assumption are compared. In addition, the volumes of the specimens are calculated using the measured specimen dimensions to show the effect of uniaxial compression on volume. Tests were performed at different stretch rates to show the synchronization capability of the proposed device at varied stretch rates.

Figure 6 presents comparative results as obtained in NR-I tested at a 0.001/s stretch rate. Figure 6*a* illustrates the difference between the measured and the incompressibility-assumption predicted Lambda-2 (λ_2) histories. The measured Lambda-2 history is found to be much lower than that predicted by the incompressibility assumption. This clearly indicates the compressibility of the specimens. Figure 6*b* gives the Cauchy stress-stretch relations as obtained from the measurement and the incompressibility assumption prediction. Here the measured Cauchy stress values are found to be higher than those obtained from the prediction.

Finally, to show the extent of volume change under uniaxial compression, Lambda-1 (λ_1) versus volume is plotted in Fig. 6*c*. The figure clearly indicates the decrease of volume with increasing applied vertical stretch (λ_1). It was found that NR-I is compressed by 4.1 % of its initial volume at 45 % compressive strain (0.55 stretch). This change in the volume is much lower than that obtained from the quantitative SEM observation on NR-I subjected to in situ tension. In that case, higher compressibility was noticed by a reduction of 9.6 % of void area at 1.4 stretch (40 % tensile strain). To explain this difference in the volume changes, it can be noted that, when a specimen is subjected to a uniaxial tensile stretch (λ_1), it undergoes compression in the other two directions (λ_2 and λ_3). On the other hand, in the case of uniaxial compression (λ_1), the specimen in the other two directions (λ_2 and λ_3) suffers extension. Hence, the compressibility feature in uniaxial loading should be more prominent in the tension regime than in the compression. The corresponding results for NR-II at a 0.075/s stretch rate and for HDR at a 0.001/s stretch rate are plotted in Figs. 7 and 8, respectively. When compared between the specimens, NR-II and HDR were found to be compressed by 2.9 % and 1.1 % of their respective initial values at 50 % compressive strain (0.50 stretch). However, when the Lambda-2 histories of NR-I and NR-II are compared (Fig. 6*a* and 7*a*), NR-II shows a larger difference between the measured Lambda-2 values than those obtained from incompressibility assumption. This may be due to the difference in applied strain rates for the two specimens. In case of NR-I, a strain rate of 0.001/s gives a response at the neighborhood of equilibrium state, while in NR-II at 0.075/s an instantaneous response is obtained [14]. In addition, the variation of carbon filler content in the microstructures of NR-I and NR-II may also be a factor in displaying a varied compressibility property.

Summary

Rubbers are usually considered as incompressible materials. Hence in mechanical testing, the true stress can be readily calculated under the incompressibility assumption to predict the deformed cross section of the specimen. However, there are cases

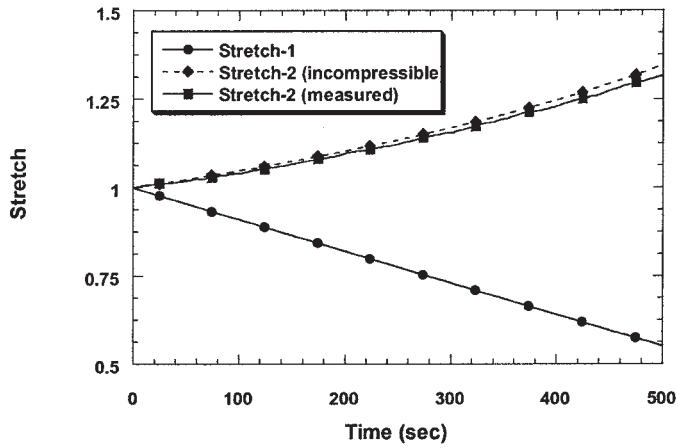

(a)

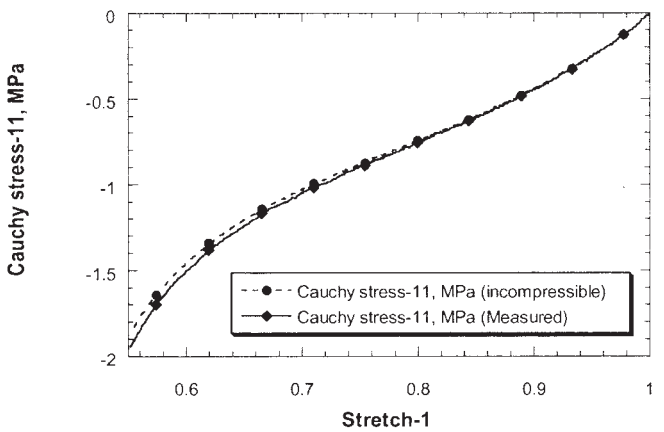

(b)

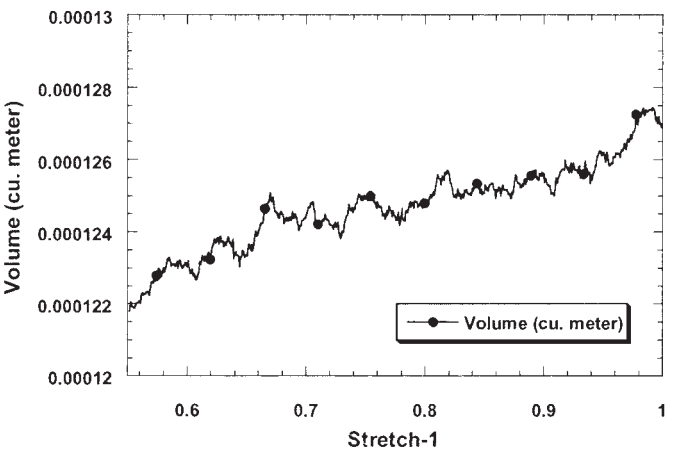

(c)

FIG. 6—*Mechanical test on NR-I subjected to monotonic compression. (a) Applied stretch, Lambda-1 (λ_1) history and corresponding Lambda-2 (λ_2) histories as obtained from incompressibility assumption and lateral deformation measurement, (b) Cauchy stress-11 versus Lambda-1 (λ_1) responses as obtained from incompressibility assumtion and lateral displacement measurement, (c) Change in volume due to the application of Lambda-1 (λ_1).*

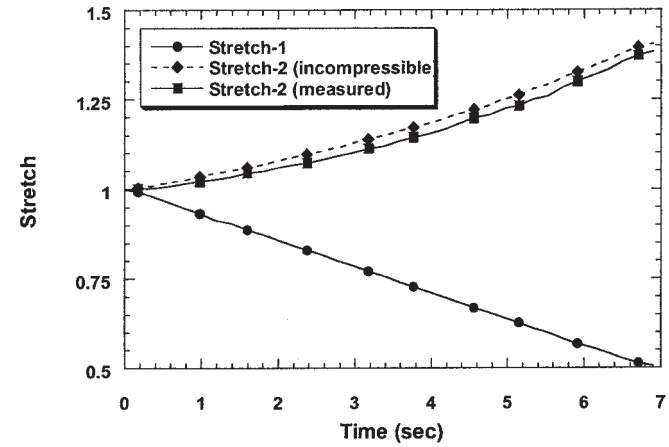

(a)

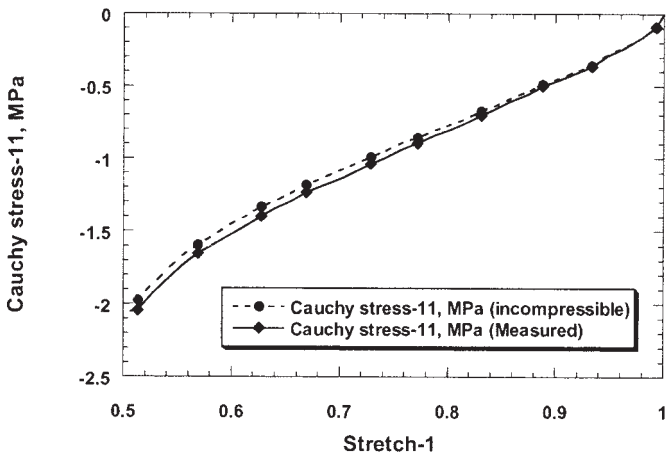

(b)

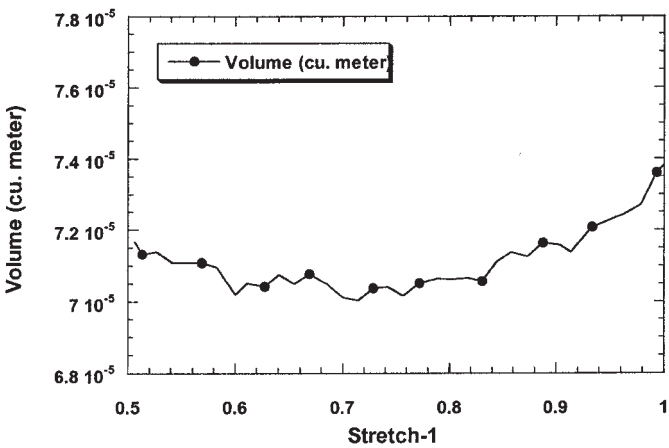

(c)

FIG. 7—*Mechanical test on NR-II subjected to monotonic compression. (a) Applied stretch, Lambda-1 (λ_1) history and corresponding Lambda-2 (λ_2) histories as obtained from incompressibility assumption and lateral deformation measurement, (b) Cauchy stress-11 versus Lambda-1 (λ_1) responses as obtained from incompressibility assumtion and lateral displacement measurement, (c) Change in volume due to the application of Lambda-1 (λ_1).*

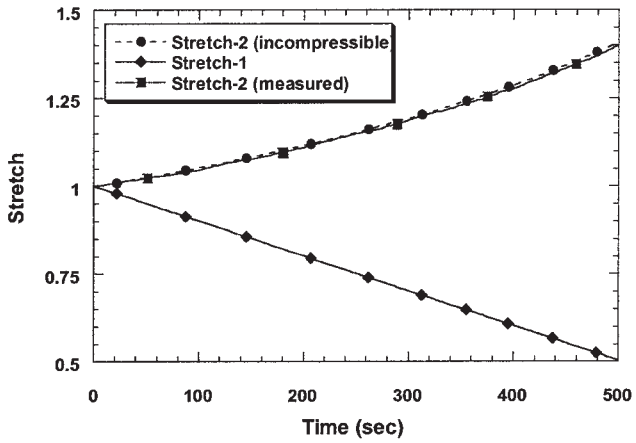

(a)

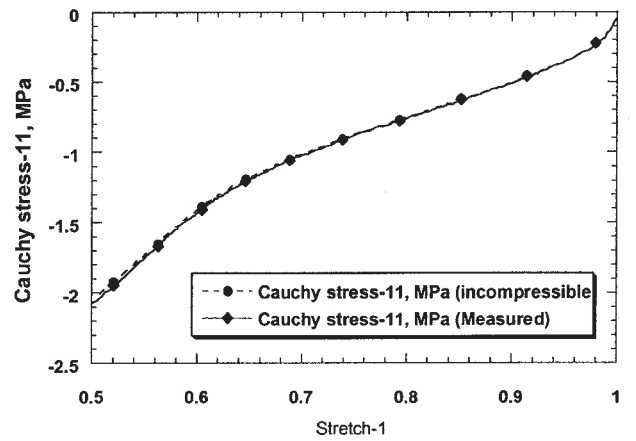

(b)

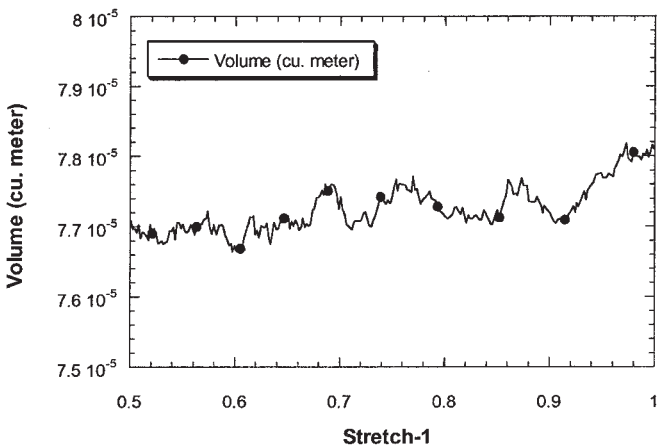

(c)

FIG. 8—*Mechanical test on HDR subjected to monotonic compression. (a) Applied stretch, Lambda-1 (λ_1) history and corresponding Lambda-2 (λ_2) histories as obtained from incompressibility assumption and lateral deformation measurement, (b) Cauchy stress-11 versus Lambda-1 (λ_1) responses as obtained from incompressibility assumtion and lateral displacement measurement, (c) Change in volume due to the application of Lambda-1 (λ_1).*

where rubbers under large strains can suffer considerable volumetric change. This notion has been clarified by considering the microstructural deformation of a void-filled natural rubber specimen. An experimental setup consisting of a mechanical boom device and a laser transducer has been designed and constructed to measure the deformed cross section of rubbers subjected to uniaxial compression. The measurements obtained from the mechanical tests of three different specimens at different stretch rates have shown the applicability of the device. Although natural rubbers and high damping rubber were used as specimens in this study to display the capability of the device, the device will also be useful in measuring the deformed cross section of other types of highly deformable solids subjected to uniaxial loading.

Acknowledgments

The authors are indeed grateful to Professor H. Horii, Department of Civil Engineering, University of Tokyo, Japan, for his valuable comments and suggestions and particularly for extending the experimental facilities of his laboratory to carry out the mechanical tests of the investigation. The authors gratefully acknowledge the kind cooperation extended by the Yokohama Rubber Co. by providing test specimens. The cooperation offered by the Active Co., Ltd., Japan in manufacturing the mechanical jig is gratefully acknowledged. The authors also sincerely recall the funding provided by the Japanese Ministry of Education, Science, Sports and Culture as Grant-in-Aid for Scientific Research (C) (No. 12650457) to carry out this research.

References

[1] Meinecke, E. A. and Taftaf, M. I., "Effect of Carbon Black on the Mechanical Properties of Elastomers," *Rubber Chem. Technol.*, Vol. 61, 1987, pp. 534–547.

[2] Hamed, G. R. and Hatfield, S., "On the Role of Bound Rubber in Carbon Black Reinforcement," *Rubber Chem. Technol.*, Vol. 62, 1988, pp. 143–156.

[3] Wischt, C. E., *The Effect of Carbon Black on Elastic and Viscoelastic Properties of Elastomers*, PhD Thesis, University of Akron, OH, 1998.

[4] Kelly, J. M., *Earthquake Resistant Design with Rubber*, Springer-Verlag, London, 1997.

[5] Mooney, M., "A Theory of Large Elastic Deformation," *J. Appl. Phys.*, Vol. 11, 1940, pp. 582–592.

[6] Rivlin, R. S. and Saunders, D. W., "Large Elastic Deformations of Isotropic Materials VII. Experiments on the Deformation of Rubber," *Phil. Trans. Roy. Soc.*, Vol. 243, 1951, pp. 251–288.

[7] Lambert-Diani, J. and Rey, C., "New Phenomenological Behavior Laws for Rubbers and Thermoplastic Elastomers," *Eur. J. Mech. A/Solids*, Vol. 18, 1999, pp. 1027–1043.

[8] Bergstrom, J. S. and Boyce, M. C., "Constitutive Modeling of the Large Strain Time-Dependent Behavior of Elastomers," *J. Mech. Phys. Solids*, Vol. 46, 1998, pp. 931–954.

[9] Bergstrom, J. S. and Boyce, M. C., "Mechanical Behavior of Particle Filled Elastomers," *Rubber Chem. Technol.*, Vol. 72, 2000, pp. 633–656.

[10] Peeters, F. J. H. and Kussner, M., "Material Law Selection in the Finite Element Simulation of Rubber-like Materials and its Practical Application in the Industrial Design Process," *Constitutive Models for Rubber*, A. Dorfmann & A. Muhr, Eds., A. A. Balkema, Rotterdam, 1999, pp. 29–36.

[11] Cornwell, L. R. and Schapery, R. A., "SEM Study of Microcracking in Strained Solid Propellant," *Metallography*, Vol. 8, 1975, pp. 445–452.
[12] Herrmann, L. R., Hamidi, R., Shafigh-Nobari, F., and Lim, C. K., "Nonlinear Behavior of Elastomeric Bearings. I: Theory," *J. Engrg. Mech., ASCE*, Vol. 114, 1988, pp. 1811–1830.
[13] Herrmann, L. R., Ramaswamy, A., and Hamidi, R., "Analytical Parameter Study for Class of Elastomeric Bearings," *J. Struct. Engrg, ASCE*, Vol. 115, 1989, pp. 2415–2434.
[14] Amin, A. F. M. S., Alam, M. S. and Okui, Y., "An Improved Hyperelasticity Relation in Modeling Viscoelasticity Response of Natural and High Damping Rubbers in Compression: experiments, parameter identification and numerical verification," *Mechanics of Materials*, Vol. 34, 2002, pp. 75–95.
[15] Amin, A. F. M. S., *Constitutive Modeling for Strain-rate Dependency of Natural and High Damping Rubbers*, Ph. D. Thesis, Saitama University, Japan, 2001.
[16] Kugler, H. P., Stacer, R. G., and Steimle, C., "Direct Measurement of Poisson's Ratio in Elastomers," *Rubber Chem. Technol.*, Vol. 63, 1989, pp. 473–487.
[17] Fishman, K. L. and Machmer, D., "Testing Techniques for Measurement of Bulk Modulus," *Journal of Testing and Evaluation*, Vol. 22, 1994, pp. 161–167.
[18] Migwi, C. M., Darby, M. I., Wostenholm, G. H., and Yates, B., "A Method of Determining the Shear Modulus and Poisson's Ratio of Polymer Materials," *J. Mater. Sci.*, 1993, pp. 3430–3432.
[19] Peng, S. H., Shimbori, T., and Naderi, A., "Measurement of Elastomer's Bulk Modulus by Means of a Confined Compression Test," *Rubber Chem. Technol.*, Vol. 67, 1994, pp. 871–879.
[20] Arruda, E. M., and Boyce, M. C., "A Three-dimensional Constitutive Model for the Large Stretch Behavior of Rubber Elastic Materials," *J. Mech. Phys. Solids*, Vol. 41, 1993, pp. 389–412.
[21] Lion, A., "A Constitutive Model for Carbon Black Filled Rubber: Experimental investigations and mathematical representation," *Continuum Mech. Thermodyn.*, Vol. 8, 1996, pp. 153–169.
[22] Boyce, M. C. and Arruda, E. M., "Constitutive Models of Rubber Elasticity: A review," *Rubber Chem. Technol.*, Vol. 73, 2000, pp. 504–523.
[23] ASTM Standard D 412-98a, Standard Test Methods for Vulcanized Rubber and Thermoplastic Elastomers-Tension, *Annual Book of ASTM Standards*, vol. 09.01, ASTM International, West Conshohocken, PA, 2002.
[24] Anand, L., "A Constitutive Model for Compressible Elastomeric Solids," *Computational Mechanics*, Vol. 18, 1996, pp. 339–355.
[25] Peng, S. H. and Chang, S. H.,"A Compressible Approach in Finite Element Analysis of Rubber Elastic Materials," *Comput. Struct.*, Vol. 62, 1997, pp. 573–593.
[26] Scion Image, *User Manual*, Scion Corporation, USA, 2000.
[27] Mullins, L., "Softening of Rubber by Deformations," *Rubber Chem. Technol.*, Vol. 42, 1969, pp. 339–362.
[28] Yeoh, O. H., "Characterization of Elastic Properties of Carbon-black Filled Rubber Vulcanizates," *Rubber Chem. Technol*., Vol. 63, 1990, pp. 792–805.
[29] Yamashita, Y. and Kawabata, S., "Approximated Form of the Strain Energy Density Function of Carbon-black Filled Rubbers for Industrial Applications," *J. Soc. Rubber Ind. (Jpn)*, Vol. 65, No. 9, 1992, pp. 517–528 (in Japanese).
[30] Lion, A., "A Physically Based Method to Represent the Thermo-mechanical Behavior of Elastomers," *Acta Mechanica*, Vol. 123, 1997, pp. 1–25.
[31] Miehe, C. and Keck, J., "Superimposed Finite Elastic-viscoelastic-plastoelastic Stress Response with Damage in Filled Rubbery Polymers. Experiments, Modeling and Algorithmic Implementation," *J. Mech. Phys. Solids*, Vol. 48, 2000, pp. 323–365.